

SIMULATION, DESIGN, AND VERIFICATION OF AN ELECTRIFIED BICYCLE ENERGY MODEL

Matt Barnes

Department of Mechanical Engineering
The Pennsylvania State University
University Park, PA 16801
mjb5497@psu.edu

Sean Brennan

Department of Mechanical Engineering
The Pennsylvania State University
University Park, PA 16801
sbrennan@psu.edu

ABSTRACT

Vehicle electrification is an increasingly popular design strategy for improving efficiency and reducing operating costs. This study uses an experimental and model-based approach to quickly and easily predict and optimize the efficiency of an electric bicycle system based on selection of critical parameters, including motor efficiency curves, rider behavior, mass, aerodynamics, and tire performance. The model is used to guide the construction of an electrified bicycle system to achieve the highest energy consumption performance among design alternatives. Tests of power consumption in actual usage show good agreement between the design predictions and measured performance.

INTRODUCTION

Electrified vehicles reduce local pollution effects and can marginally decrease net energy consumption, providing advantages to internal combustion systems [1-5]. Further, conventional bicycles are an inexpensive and accessible mode of transportation, but are rarely used in lieu of automobiles because they are comparably slow, have limited cargo space, and require human effort which can cause undesirable perspiration while commuting. This project analyzes the energy model and experimental performance of a trailered electrical propulsion system that converts a bicycle into an electrically propelled vehicle. It thus takes advantage of the highly efficient nature of bicycles and benefits of electrification, while offering an appealing alternative to automobiles for typical daily commuting and car usage [6].

The design studied in this work is based on a trailer system that attaches and detaches easily from a bicycle, and provides pushing power, payload storage, and electrical battery energy all from a single unit, as seen in Fig. 1. When detached, the bicycle can be used as a traditional bicycle, thereby eliminating downtime during charging. If the user has access to multiple trailers, the depleted trailers may be quickly interchanged with



FIGURE 1. PROTOTYPE ELECTRIC BICYCLE TRAILER

fully charged ones for continuous electrical operation. When attached, the bicycle can be propelled entirely by electric assist, manual input, or any combination of the two, thus allowing the rider to choose his/her contributions to vehicle energy, and providing a fail-safe means of reaching a destination in the case of electric systems failures. Desired electric assist is easily manipulated using a twist-grip throttle located on the handlebars in a style similar to currently-marketed electric scooters. The trailer not only provides the electrical propulsion and energy storage, but provides additional spare storage space to carry up to 30kg (~70lbs) of luggage, groceries, etc.

Prior to conducting any testing, the safety of similar systems was investigated. Transportation data shows electrified bicycles are dramatically safer than automobiles, and only marginally more dangerous than conventional bicycles. In urban China, both electrified bicycle fatality and injury rates per kilometer per passenger are one to two orders of magnitude lower than automobiles [7]. Though no safety data exists for bicycle trailers, the prevalence of commercial trailers for child carrying purposes leads the authors to believe the trailer is sufficiently safe. Regardless, the model presented in this paper is not limited to trailered systems – it is applicable to all electric bicycles.

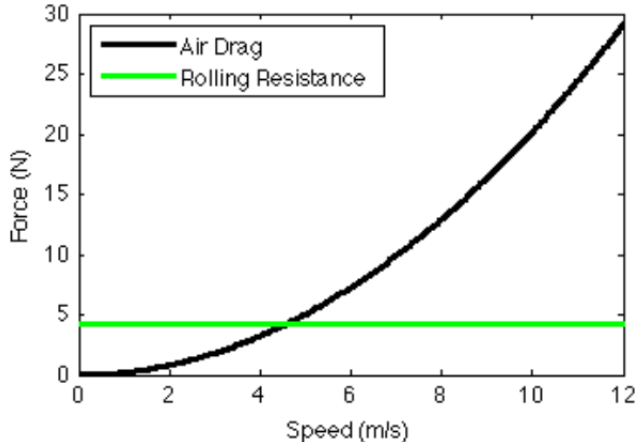


FIGURE 2. PREDICTED OPPOSING FORCES

To optimize the performance of the system, an experimental and model-based approach was used in the trailer design. The goal is to maximize and predict the efficiency of the pre-built system using dynamometer tests of commercially available brushless DC motors, the riding patterns of a sample of electric bike users, and published rolling resistance and wind drag coefficients. Next, a physical prototype was constructed using these optimized criteria, and tests of power consumption in actual usage show good agreement between the design predictions and measured performance. Using the Greenhouse Gases, Regulated Emissions, and Energy Use in Transportation (GREET) model published by Argonne National Laboratory, the upstream energy and emission costs were calculated for comparison to conventional automobiles [8]. The results, presented shortly, show that even without any pedaling by the user, the measured efficiency of 37.1 kJ/km corresponds to 2.95% of the net greenhouse gas (GHG) emissions and 2.75% of the fuel consumption of a typical US passenger vehicle.

THEORY AND RELATED LITERATURE

The basis of the model used to design an optimized efficiency is the analysis of forces opposing motion. For cycling on level ground, the air and rolling resistance compromise the majority of forces [9]. Even in cases with hills, as long as there is zero net elevation change, and as long as rider speed behavior is consistent, then the effects of hills on net energy consumption can be largely ignored.

Air Resistance

The drag force is a function of a coefficient C , frontal area A_F , air density ρ , and velocity of the air relative to the bike V_{air} [10].

$$F_D = \frac{1}{2} \rho A_F C V_{air}^2 = C_D V_{air}^2 \quad (1)$$

In this study, the velocity of the air relative to the ground is assumed to be zero. Therefore, the relative air velocity is obtained by the velocity of the bicycle.

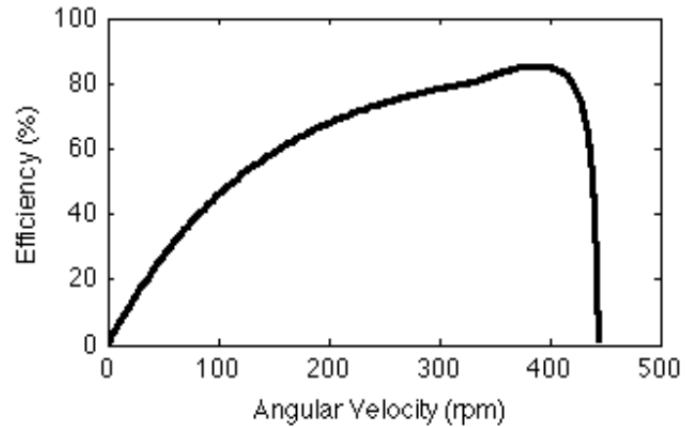


FIGURE 3. MOTOR EFFICIENCY CURVE OF NINECONT2805

Many of these parameters have been measured in previous studies. For bicycle riders in a fully dropped racing position, the product of the $\frac{1}{2}\rho$, A_f , C coefficients, which we define as the generic air drag coefficient C_D , were experimentally determined by di Prampero et al. to equal $0.202 \text{ kg}\cdot\text{m}^{-1}$ [9]. The trailer, which rides in the wake of the bicycle, adds additional width and slightly increases the frontal area. However, this will be relatively small, so the design analysis initially ignores the aerodynamic effects of the trailer.

Rolling Resistance

The rolling resistance F_{RR} is a function of the rolling resistance coefficient C_{RR} and normal force F_N [11]

$$F_{RR} = C_{RR} F_N = C_{RR} m g \quad (2)$$

The C_{RR} value for bicycle road tires, which are similar to the ones used in this study, were determined by Burke to be approximately .0039 [12]. Rolling resistance is quickly overpowered by air resistance as velocity increases, as shown in Fig. 2.

Net Force

The summation of forces on the system shows

$$m a = F_{motor} - F_D - F_{RR} \quad (3)$$

where F_{motor} is the pushing force supplied by the motor. Since the vehicle starts and ends at rest, the net acceleration is zero. Thus, net energy consumption due to acceleration should be minimal and is neglected from Eq. (3), leaving

$$F_{motor} = F_D + F_{RR} \quad (4)$$

This assumption will be justified in a later section with real-time analysis.

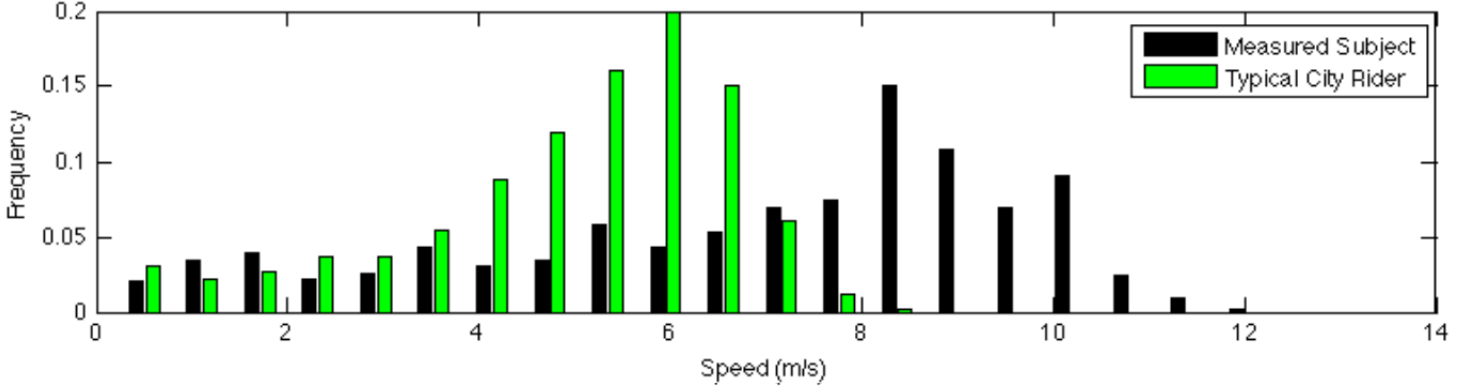


FIGURE 4. HISTOGRAM OF ELECTRIC BICYCLE RIDER SPEED FREQUENCIES

Energy

The efficiency of the system will be expressed in terms of energy consumption per distance. This is a reciprocal of the automobile efficiency standard miles per gallon. These measurements enable a quantitative optimization of the system's performance.

Elementary mechanics tells us the work performed by the motor, W_{motor} , is equal to

$$W_{motor} = F_{motor}d \quad (5)$$

where d is the distance traveled. Thus mechanical work per distance is equal to the pushing force supplied by the motor.

Energy consumption is obtained by a measurement of electrical energy, of which a portion is converted to useful work and the remainder is dissipated as waste (e.g. heat). The relationship between electrical energy and work is described as

$$E_{elec}\eta(\omega) = W_{motor} \quad (6)$$

where $\eta(\omega)$ is the efficiency of the motor as a function of angular velocity, as exemplified in Fig. 3. Energy used by the motor controller and resistive loss in connecting wires is assumed to be negligible. The motor efficiency is provided by the manufacturer for most motors. The angular velocity of the motor can be expressed as a function of bicycle ground speed by:

$$\omega = 2rG_RV_{ground} \quad (7)$$

where r is the wheel radius and G_R is the gear ratio. The hub motors used in this study are directly attached to the wheel and therefore have a direct drive 1:1 gear ratio. The trailer uses a 254 mm (10") radius wheel, with 23 uniformly distributed Hall Effect sensors for determining position, speed, and acceleration.

Combining Eq. (1), Eq. (2) and Eq. (4) to (7) with a motor efficiency curve $\eta(\omega)$ yields the instantaneous electrical energy

use per distance

$$\left(\frac{E_{elec}}{x}\right)_i = \frac{\frac{1}{2}\rho A F C_D V_{ground}^2 + C_{RR} F_N}{\eta(2rG_R V_{ground})} \quad (8)$$

Typical Riding Patterns

One of this study's goals is to create a model for selecting an appropriate motor and battery to maximize efficiency and accurately predict range of an electrified vehicle for a typical rider. Since the efficiency of the motor is dependent of rider speed, typical rider speeds must be determined. A study of typical city electric bicycles riders in the Chinese cities of Shanghai and Kunming conducted by Cherry was used to create a speed histogram, seen in Fig. 4 [7].

For each speed in the histogram, the energy use per distance is calculated using Eq. (8). Thus, the speed histogram can be converted to an energy use per distance histogram. Determining the average electrical energy per distance for the typical rider is readily done by summing all the bins of this histogram

$$\left(\frac{E_{elec}}{x}\right)_{ave} = \sum_{i=V_{min}}^{V_{max}} \left[\left(\frac{E_{elec}}{x}\right)_i f(V_{ground,i}) \right] \quad (9)$$

where $f(V_{ground})$ is the frequency of V_{ground} for the typical city rider.

This analysis is optimistic in that it excludes any energy lost due to braking. For a typical bicycle commuter, the energy lost to braking is normally around 8% of the total energy expended [12]. Therefore, the average electrical energy per distance including braking is

$$\left(\frac{E_{elec}}{x}\right)_{ave} = \left(\frac{1}{1-E_{brake}}\right) \sum_{i=V_{min}}^{V_{max}} \left[\left(\frac{E_{elec}}{x}\right)_i f(V_{ground,i}) \right] \quad (10)$$

where E_{brake} is .08, a representative of the typical fraction of energy lost due to braking for bicycles. Future work will analyze the efficiency benefits of regenerative braking, a feature which was disabled on the current prototype for the purposes of this study.

Optimal motor selection will occur by iteration of the

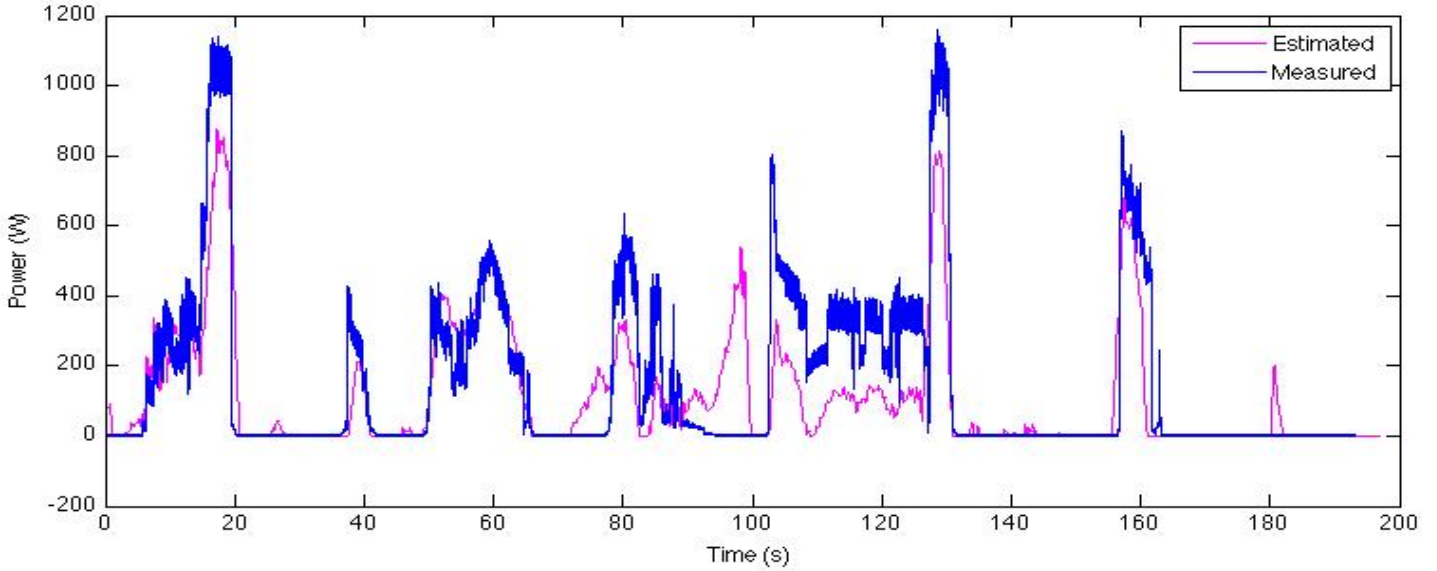


FIGURE 5. REAL-TIME ANALYSIS OF PREDICTED AND MEASURED POWER

model with a selection of efficiency curves for commercially available motors. The motor with the lowest predicted energy consumption per distance is the most efficient motor for the typical city rider.

Real-time Analysis

Conducting real-time comparison of measured and predicted energy consumption enables a more in-depth analysis of model performance. In order to accurately predict power draw, motor forces due to vehicle acceleration also need to be considered. Power will increase during periods of acceleration and decrease during periods of deceleration. In lieu of the simplified Eq. (4), real-time power analysis will use the more comprehensive Eq. (3). This was not necessary for typical rider net energy, nor was it possible due to the lack of published acceleration data.

Further, real-time analysis enables the reconstruction of Fig. 2 for measured data. This is most easily done with coast-down tests, where the subject decelerates from maximum velocity to a near stop without applying any motor force. Thus, for coast down tests, Eq. (3) simplifies to

$$ma = -F_D - F_{RR} = -\frac{1}{2}\rho A_F C_D V_{air}^2 - C_{RR} F_N \quad (11)$$

A second order polynomial curve-fit will allow calculation of measured drag coefficients for comparison to literature values.

METHODS

Of the sample of selected commercially available motors, the Nine Cont 2805 hub motor had the lowest energy use per distance predicted by Eq. (10) for a typical city rider, and was purchased to conduct physical testing. Typically, bicycles use a single Hall Effect sensor to measure speed. The motor in this

study has 23 Hall Effect sensors for accurately controlling speed, and were conveniently accessed to provide distance measurements. For an inflated tire, the distance between pulses was calibrated using measured number of pulses over a measured distance, for normal riding. Incremental change in distance and time were recorded at every Hall Effect sensor pulse by using interrupts into an embedded computing system.

Speed was determined by dividing change in distance by change in time between measurements. A 2 second moving average filter was applied to smooth the data prior to differentiating again to determine acceleration. Finally, a 1 second moving average filter was applied to the acceleration data. Other filtering approaches such as Butterworth and median were not chosen because they inherently skewed data summations used for net energy calculations.

For real-time analysis, small negative predicted power and energy values were observed during periods of coasting. Regenerative braking was disabled during testing, so reverse energy flow could not occur. These negative values were set equal to zero by assuming acceleration forces to be accurate, and temporarily increasing air drag and rolling resistance values.

Actual current and voltage levels were recorded at 1000 Hz using a highly accurate power monitoring device used for battery condition monitoring. Power at every sample point was determined according to

$$P = i \cdot v \quad (12)$$

where P is power draw, i is current, and v is voltage. Measured energy was determined by integrating power with respect to time.

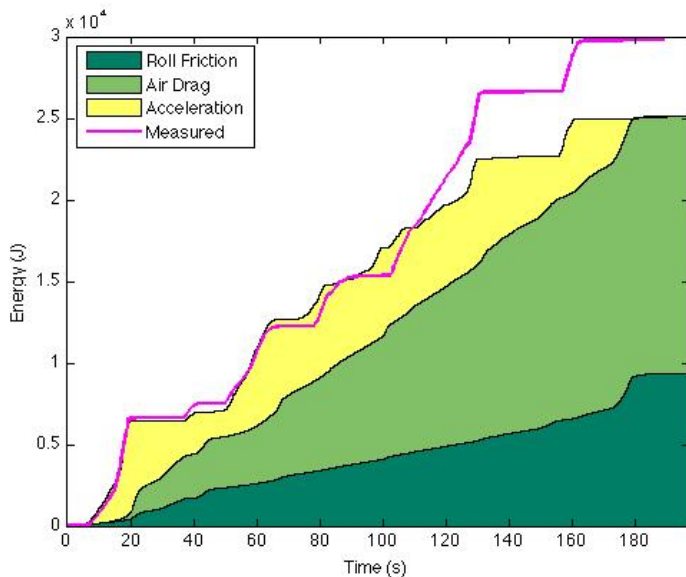


FIGURE 6. CUMULATIVE ENERGY BREAKDOWN

To conduct the study, the subject rode random routes about Centre County, PA on typical asphalt roads. Coast-down tests were conducted on a straight level course at the Penn State Test Track Facility. In accordance with the literature's drag coefficients, the rider rode in the "fully dropped" position. The combined mass of the bicycle, trailer, and rider system was 108 kg. Eleven kilometers of data were logged for this study.

RESULTS AND DISCUSSION

Rider Behavior

For the purposes of comparing predicted and measured efficiencies, a second speed histogram was generated specifically for the subject's riding patterns, shown in Fig. 4. Not surprisingly, the subject riding in the less-congested test area rode faster than typical city riders reported in literature. At faster speeds there is greater wind resistance, shown in Fig. 2, thus increasing the energy use per distance.

Applying this new histogram and the Nine Cont 2805 efficiency curve to Eq. (10), the net energy consumption per distance was predicted specifically for the subject and is presented shortly along with the measured data. Consideration of driving environment and rider characteristics significantly change efficiency and are critical when designing electrified vehicles.

Predicted and Measured Efficiency

One expects the measured energy use to be larger than predicted energy use because of neglected model terms including: additional drag caused by the trailer, controller power draw, resistive losses in connecting wires, and variable headwind. Effort was made by subjects to minimize the effects of these factors by riding on level ground during calm weather conditions. Unavoidably, these factors still caused additional

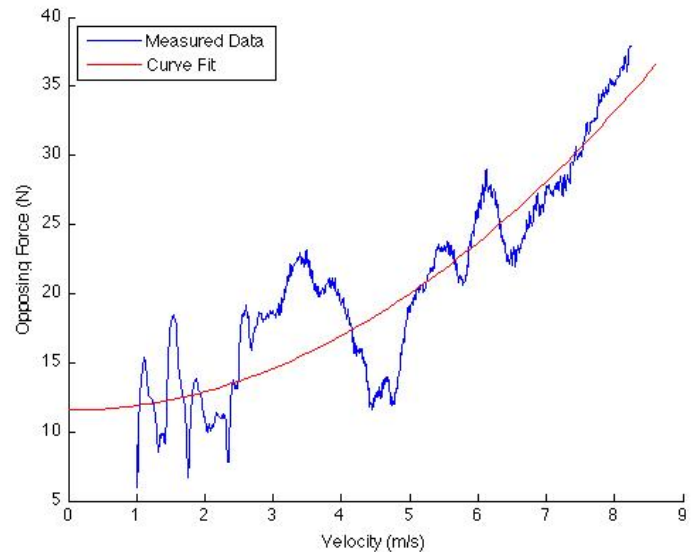


FIGURE 7. COAST-DOWN TEST

energy usage, resulting in a predicted energy use of 31.1kJ/km, 16% lower than the measured energy use of 37.1kJ/km.

To compare the measured efficiency of the electric bicycle to automobiles, the upstream GHG and fuel costs were determined using the GREET model [8]. Given a charger efficiency of 83%, the optimized electrified bicycle results in 111 kJ/km of net energy consumption and 14.1 g/km of CO₂ equivalent GHGs, representing 2.75% and 2.95% of typical US passenger automobiles, respectively.

Real-time Analysis

A more thorough understanding of the results is evident by examining real-time data, a small selection of which is shown in Fig. 5. Note the high tracking accuracy until approximately $t=65s$. A slight downgrade in the road until $t=100s$ and upgrade until $t=125s$ causes high and low estimated energy predictions, respectively. Future work will incorporate elevation change to improve real-time model accuracy.

Cumulative energy consumption breakdowns are shown in Fig. 6. Note that, by the end of the trip, the energy due to the integrated power from acceleration returns to less than 0.5% of the total energy. This is expected, as acceleration forces are fully expected to overcome drag forces and rolling friction. If one only needs to know end-of-trip energy utilization, one can simply use velocity histograms for typical rider behavior. As expected, air drag encompasses the majority of energy dissipation at 63%, with rolling resistance encompassing 37%.

Results of the coast-down test are shown in Fig. 7. Due to additional resistance forces caused by the trailer, both rolling resistance and air drag are higher than those reported in the literature. A second order polynomial curve fit shows the measured C_D and C_{RR} values are 0.3303 kg·m⁻¹ and 0.010, respectively. The measured rolling resistance coefficient is over

twice that reported in the literature due to the large idling torque in the motor and the additional BMX-type trailer tire. The measured air drag coefficient is approximately 60% larger than that in the literature.

Applying the measured drag coefficients to the energy model results in a predicted energy use 30% larger than measured. The large discrepancy leads one to believe the measured C_D and C_{RR} values are inaccurate. Coast-down tests may not be a good choice for electric hub motor systems due to the idling torque, which does not exist when the motor is active during the majority of normal use.

CONCLUSIONS

The electrified vehicle energy model developed in this study was used to predict vehicle efficiency and optimal motor selection. The models were used to design and construct a novel electric bicycle trailer. Tests of a prototype in actual usage show good agreement between designed predictions and measured performance, with less than 20% error between model and experiment. The energy outputs are dominated by wind resistance and rolling resistance, which is expected for electric bicycles. The final estimated efficiency, GHG emissions, and upstream fuel consumption of the system suggests electric bicycles are a particularly efficient alternative to conventional automobiles. The model results are useful for analyzing and optimizing power and energy requirements for any number of rider behaviors, environments, tires, aerodynamic drag parameters, and masses.

REFERENCES

- [1] Chan, C. C., 2007, "The State of the Art of Electric, Hybrid, and Fuel Cell Vehicles." *Proceedings of the IEEE* **95**(4), pp. 704-718.
- [2] Elgowainy, A., 2009, "Well-to-Wheels Energy Use and Greenhouse Gas Emissions Analysis of Plug-in Hybrid Electric Vehicles," DOE Argonne National Laboratory Energy Systems Division, Lemont, IL.
- [3] Emadi, A., Lee, Y.J., and Rajashekara, K., 2008, "Power Electronics and Motor Drives in Electric, Hybrid Electric, and Plug-in Hybrid Electric Vehicles," *IEEE Transactions on Industrial Electronics* **55**(6), pp. 2237-2245.
- [4] Howey, D. A., et al, 2011, "Comparative Measurements of the Energy Consumption of 51 Electric, Hybrid and Internal Combustion Engine Vehicles," *Transportation Research Part D*, **16**(6), pp. 459-464.
- [5] Stephan, C. H., and Sullivan, J, 2008, "Environmental and Energy Implications of Plug-in Hybrid-Electric Vehicles." *Environmental Science & Technology* **42**(4) pp. 1185-1190.
- [6] Muetze, A., and Ying, C.T., 2005, "Electric Bicycle - A Performance Evaluation," *IEEE Industry Applications Magazine*, **13** (4), p. 12.

- [7] Cherry, C.R., 2007, "Electric Two-Wheelers in China," Ph.D. Thesis, Department of Civil and Environmental Engineering, University of California Berkeley.
- [8] Wang, M., 2011, "Greenhouse Gases, Regulated Emissions, and Energy Use in Transportation," DOE Argonne National Laboratory Energy Systems Division, Lemont, IL.
- [9] di Prampero, P.E., Cortili, G., Mognoni, P., and Saibene, F., 1979, "Equation of Motion of a Cyclist," *Journal of Applied Physiology*, **47**(1), pp. 201-206.
- [10] Cengel, Y.A., and Cimbala, J.M., 2010, *Fluid Mechanics: Fundamentals and Applications*, McGraw-Hill, New York.
- [11] National Research Council, 2006, "Tires and Passenger Vehicle Fuel Economy," *Transportation Research Board Special Report 286*, Washington, DC.
- [12] Burke, E.R., 1986, *Science of Cycling*, Leisure Press, Illinois.